

# The stability of rotating-disc boundary-layer flow over a compliant wall. Part 2. Absolute instability

By A. J. COOPER<sup>†</sup> AND PETER W. CARPENTER

Department of Engineering, University of Warwick, Coventry, CV4 7AL, UK

(Received 23 May 1996 and in revised form 3 July 1997)

A numerical study has been undertaken of the influence of a compliant boundary on absolute instability. In a certain parameter range absolute instability occurs in the boundary layer on a rotating disc, thereby instigating rapid transition to turbulence. The conventional use of wall compliance as a laminar-flow control technique has been to lower growth rates of convective instabilities. This has the effect of reducing amplification of disturbances as they propagate downstream. For absolute instability, however, only the suppression of its onset would be a significant gain. This paper addresses the question of whether passive wall compliance can be advantageous when absolute instability exists in a boundary layer.

A theoretical model of a single-layer viscoelastic compliant wall was used in conjunction with the sixth-order system of differential equations which govern the stability of the boundary-layer flow over a rotating disc. The absolute/convective nature of the flow was ascertained by using a spatio-temporal analysis. Pinch-point singularities of the dispersion relation and a point of zero group velocity identify the presence of absolute instability. It was found that only a low level of wall compliance was enough to delay the appearance of absolute instability to higher Reynolds numbers. Beyond a critical level of wall compliance results suggest that complete suppression of absolute instability is possible. This would then remove a major route to transition in the rotating-disc boundary layer.

---

## 1. Introduction

Lingwood (1995, 1996) has recently shown that absolute instability may be an important route to transition in the three-dimensional boundary layer over a rotating disc. The absolute instability arises from the coalescence of a travelling Type I cross-flow vortex and a hitherto obscure eigenmode (Type III), first identified by Mack (1985), which appears to propagate inwards and to be damped. In both her theoretical and experimental studies Lingwood triggered the disturbances impulsively. Nonetheless the existence of absolute instability could explain why a survey of a large number of previous experimental investigations of natural transition over rotating discs reveals that the transitional Reynolds numbers are centred around a value of about 513 with only a 3% scatter, as pointed out by M. Gaster (1992 private

<sup>†</sup> Present address: Department of Applied Mathematics and Theoretical Physics, University of Cambridge, Silver Street, Cambridge CB3 9EW, UK.

communication), cited in Lingwood (1995). This is in stark contrast with the laminar–turbulent transition process in other flows, such as the Blasius boundary layer, where solely convective instabilities are known to be involved.

In Part 1 (Cooper & Carpenter 1997) the effect of wall compliance on boundary-layer instability over a rotating disc was studied. Amongst other things we showed that wall compliance has a substantial stabilizing effect on the Type I cross-flow instability. This result is encouraging from the viewpoint of using wall compliance for laminar-flow control of three-dimensional boundary layers. But the promise implicit in our findings would come to nought if the Lingwood absolute instability were not also suppressed. Fortunately it is likely that if one of the coalescing eigenmodes is suppressed the absolute instability will, in fact, at the very least be postponed to a higher Reynolds number. This is in essence what is shown to happen in the present paper which investigates theoretically the effects of wall compliance on the Lingwood absolute instability.

In the interests of brevity we will not review the substantial literature on rotating-disc boundary-layer instability for both rigid and compliant walls, but rather refer the reader to Lingwood (1995, 1996) and Part 1. Similarly the details of the theoretical treatment will also be omitted since it combines those of Lingwood (1995, 1997*a*) and Part 1 which are followed closely.

Section 2 provides a brief outline of the problem. Results for rigid and compliant boundaries are presented in §3 and conclusions from the investigation are drawn in §4.

## 2. Formulation of the fluid problem

The disc is assumed to be infinite in diameter and rotating about its centre at a constant angular velocity  $\Omega$ . A cylindrical coordinate system in the rotating frame is used with radius  $r^*$ , azimuthal angle  $\theta$  and normal direction  $z^*$  and the fluid is assumed to occupy the region  $z^* > 0$ . The mean flow field is obtained from the exact similarity solution of the Navier–Stokes equations due to von Kármán (1921).

For the linear stability analysis a space–time-dependent perturbation field of infinitesimal disturbances is imposed on the mean flow field. The displacement thickness  $\delta^* = (\nu/\Omega)^{1/2}$  (where  $\nu$  is the kinematic viscosity of the fluid),  $r_e^*\Omega$  (where  $r_e^*$  is an arbitrary fixed radius) and  $\rho r_e^{*2}\Omega^2$  (where  $\rho$  is the fluid density) are used throughout to non-dimensionalize length, velocity and pressure respectively. Thus  $r = r^*/\delta^*$  is the variable non-dimensional radius and the Reynolds number

$$R = r_e^*/\delta^*$$

is the non-dimensional fixed radius.

Following linearization of the Navier–Stokes equations, slow variation of the Reynolds number with radius is ignored so that the quantity  $r$  is replaced with  $R$ . Terms of order  $R^{-2}$  and higher-order terms are subsequently neglected. The perturbation quantities are then expressed in the normal-mode form, such that they are proportional to

$$E = \exp\{i(\alpha r + \beta R\theta - \omega t)\}$$

where, in general,  $\alpha$  is the complex radial wavenumber,  $\beta$  the wholly real azimuthal wavenumber and  $\omega$  is the complex frequency of the disturbance.

This process leads to the sixth-order system of equations, originally derived by Malik, Wilkinson & Orszag (1981), which retain the effects of Coriolis acceleration

and streamline curvature and which, for present purposes, define an eigenvalue problem of the form

$$\mathcal{F}(\alpha; \beta, \omega, R) = 0.$$

The stability equations are solved using the spectral method described in Part 1. One advantage of this particular numerical method, in the context of absolute instability, is that group velocities can be calculated readily at relatively little extra cost.

The compliant wall is assumed to be an infinitely deep homogeneous viscoelastic layer and its dynamics are modelled by means of the Navier equations. As noted in Part 1, the assumption of infinite depth is not unduly restrictive since the disturbances only penetrate a finite depth of wall. This type of compliant-wall model was chosen in support of an ongoing experimental study.

There is no clearly defined manner in which to express non-dimensional shear and bulk moduli characterizing the viscoelastic material, since the obvious reference pressure of  $\rho r_e^* \Omega^2$  varies with radial location. Accordingly the theoretical problem is approached from a practical viewpoint so that a layer of fixed material properties is used and changes in wall compliance are effected by varying the rotational speed of the disc. To retain some correspondence with an ongoing experimental research project for which a soft silicone rubber is used as the compliant wall, fixed values of shear modulus,  $G_s = 1000 \text{ N m}^{-2}$  and Poisson ratio of 0.49 are taken. The length scale for the wall equations is taken to be the constant boundary-layer thickness  $\delta^*$ . Further details of the theoretical modelling of the compliant wall, including the coupling between the wall and fluid dynamics, are given in Part 1.

### 3. Analysis of absolute instability

In order to establish whether a flow is absolutely or convectively unstable a spatio-temporal analysis must be performed, where both frequency and wavenumber take complex values. The original concept of absolute and convective instability arose in the area of plasma physics (Briggs 1964; Bers 1975). Huerre & Monkewitz (1990) review developments in hydrodynamic stability theory concerning absolute and convective instabilities in spatially developing flows. The response of the flow to impulsive forcing determines whether it is absolutely or convectively unstable.

Absolute instabilities can be identified numerically by following the paths of two solution branches in the  $\alpha$ -plane. When waves propagating in opposite directions coalesce this corresponds to the crossing or intersection of the solution branches and 'pinching' is said to occur. The exact point of coalescence in the  $\alpha$ -plane is termed a pinch point. This corresponds to a singularity in the governing dispersion relation producing a branch-point singularity in the  $\omega$ -plane. Variations in flow parameters cause such pinch points to arise whereby a convectively unstable flow becomes absolutely unstable. However, certain criteria must be satisfied in order for branch-point singularities in the dispersion relation to identify correctly an absolute instability. To satisfy causality two solution branches must originate in distinct halves of the  $\alpha$ -plane at large positive  $\omega_i$  and as  $\omega_i$  is reduced coalescence should occur before  $\omega_i$  reaches zero. If  $\omega_i$  is reduced to zero before pinching occurs then the flow remains convectively unstable. This method of identifying absolute instability is known as the Briggs (1964) criterion.

Lingwood (1995) assessed the response of the flow to impulsive forcing and solved the initial boundary-value problem posed by an impulsive line forcing,  $\delta(r - r_s)\delta(t)e^{i\beta\theta}$ ,

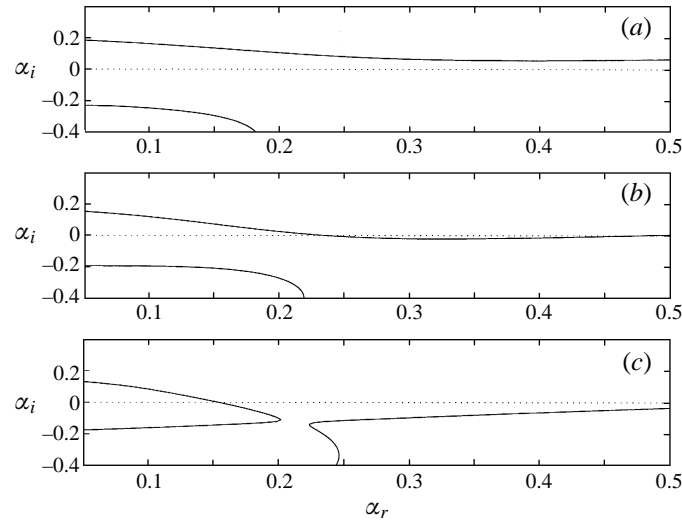


FIGURE 1. Spatial branches 1 and 3 in the  $\alpha$ -plane, for the rigid disc, with  $\beta = 0.126$  and  $R = 530$ . (a)  $\omega_i = 0.01$ , (b)  $\omega_i = 0.004$ , (c)  $\omega_i = 0.000289$ .

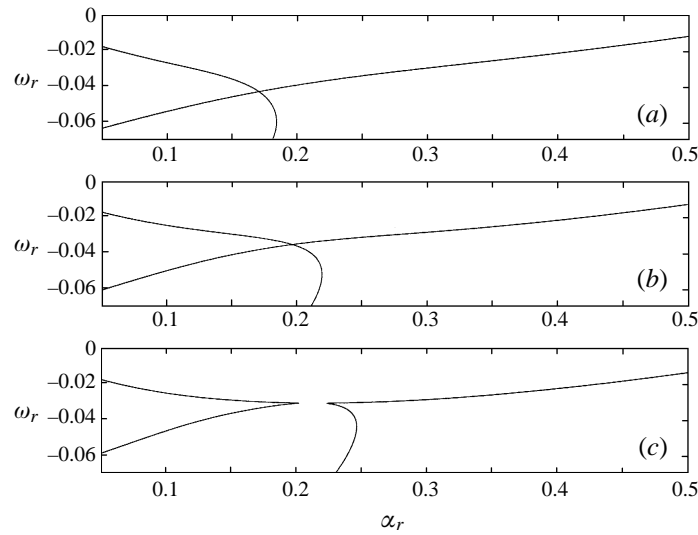


FIGURE 2. Spatial branches 1 and 3 in the  $(\omega_r, \alpha_r)$ -plane, for the rigid disc, with  $\beta = 0.126$  and  $R = 530$ . (a)  $\omega_i = 0.01$ , (b)  $\omega_i = 0.004$ , (c)  $\omega_i = 0.000289$ .

where  $\delta(r - r_s)$  and  $\delta(t)$  are the Dirac delta functions at a non-dimensional radius of  $r_s$  and at  $t = 0$  respectively. A finite range of  $\beta$  values were found to define the absolutely unstable region of the flow, but the value of  $\beta = 0.126$  has been chosen arbitrarily to demonstrate the existence of absolute instability.

### 3.1. Results for the rigid wall

Calculations for the rigid disc were performed at  $R = 530$  and results found to agree well with those of Lingwood (1995). The data take the form of eigenvalues,  $\alpha = \alpha_r + i\alpha_i$ , calculated for different values of  $\omega_r$  so that travelling modes are assumed in the analysis. Figure 1 shows the evolution of the two spatial branches as  $\omega_i$  is

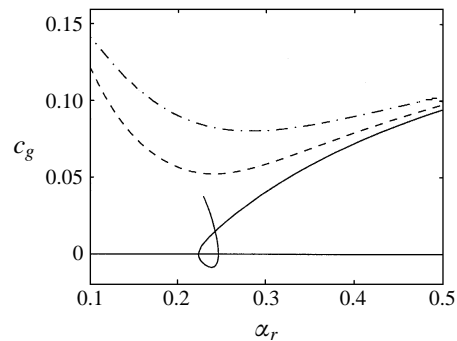


FIGURE 3. Variation of branch-1 group velocity:  $-\cdot-$ ,  $\omega_i = 0.01$ ;  $- -$ ,  $\omega_i = 0.04$ ;  $—$ ,  $\omega_i = 0.000289$ .  $\beta = 0.126$ ,  $R = 530$ .

decreased. At  $\omega_i = 0.01$  the two branches are located in opposite halves of the  $\alpha$ -plane, with branch-1 modes residing in the upper half of the  $\alpha$ -plane and branch-3 modes in the lower half<sup>†</sup>. As  $\omega_i$  is decreased the two branches begin to converge and pinching occurs around  $\omega_i = 0.000289$ . Although the exact point of coalescence is not shown, the change in structure of the two solution branches after coalescence is clearly evident. Figure 2 plots  $\omega_r$  against  $\alpha_r$ . It is noted that both solution branches in the  $\alpha$ -plane correspond to disturbances with negative frequency, or those that travel inwards. Pinching occurs in the region of  $\omega_r \approx -0.031$ . In addition to the results of Lingwood the group velocity, defined by the real part of  $\partial\omega/\partial\alpha$ , of the branch-1 mode has been calculated. Figure 3 demonstrates how the group velocity curves approach the zero point as  $\omega_i$  is reduced. The exact point of pinching, or the onset of absolute instability, is identified by a sharp cusp point in the group velocity curve, which is zero at the value of  $\alpha_r$  corresponding to the pinch point. This cusp point is necessary but not sufficient for absolute instability. After coalescence the group velocity curve loops below the zero line and this characteristic is taken to be another indication of the existence of absolute instability and is used in the compliant-wall problem to assess the convective/absolute nature of the flow. It should be noted that the Briggs criterion must be known to be satisfied before the group velocity can be used in this way to identify the existence of absolute instability.

It has been shown that branches 1 and 3 originate in opposite halves of the  $\alpha$ -plane. Therefore, for absolute instability to be suppressed a delay in the appearance of pinch points until  $\omega_i$  is zero is required.

### 3.2. Results for the compliant wall

Initially a small degree of wall compliance was considered by assuming a disc rotation speed of  $\Omega = 2.5 \text{ rad s}^{-1}$ . This is a very low rotation rate compared to experimental investigations, but theoretically results for the rigid disc are unaffected by the value of rotation rate. Given that transition occurs at  $R \approx 513$  then smaller rotation rates simply imply that transition occurs at a larger disc radius. Experimental analyses are constrained by physically reasonable disc dimensions so that high rotation rates are required if the boundary-layer stability characteristics are to be accommodated within the diameter of the disc. For the case of a compliant boundary, however, rotation rate is an important factor because it directly affects the linear speed of

<sup>†</sup> Branch 1 corresponds to the Type I instability, branch 2 (not shown) to the Type II viscous instability, and branch 3 to Type III – the third eigenmode originally discovered by Mack (1985).

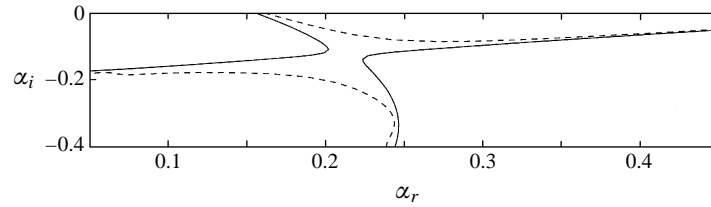


FIGURE 4. Branches 1 and 3 in the  $\alpha$ -plane with  $\beta = 0.126$ ,  $R = 530$  and  $\omega_i = 0.000289$ : —, rigid wall; - -, compliant wall at  $\Omega = 2.5 \text{ rad s}^{-1}$ .

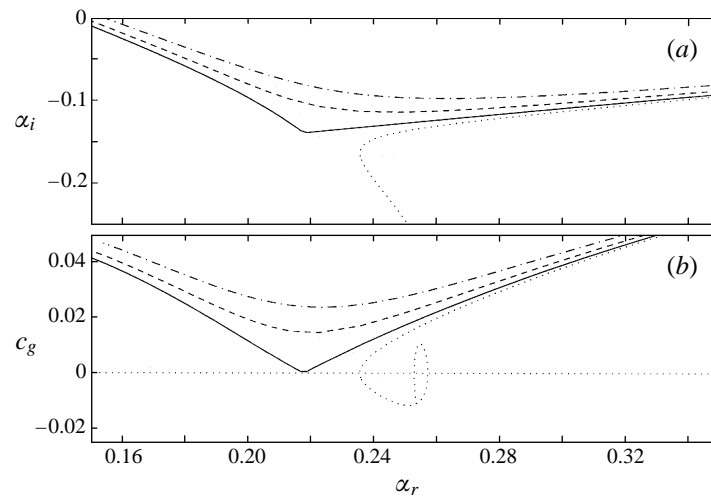


FIGURE 5. Evolution of branch 1 with Reynolds number over compliant boundary with  $\Omega = 2.5 \text{ rad s}^{-1}$ .  $\beta = 0.126$ ,  $\omega_i = 0$ . (a) Variation in the  $\alpha$ -plane, (b) variation of group velocity with  $\alpha_r$ . — · —,  $R = 540$ ; - -,  $R = 580$ ; —,  $R = 607.8$ ; ···,  $R = 625$ .

the disc at each radial location. The measure of wall compliance is related to the non-dimensional wall-stiffness parameter and at a fixed dimensional shear modulus this is inversely proportional to the square of the linear speed,  $r_e^* \Omega$ . Therefore as  $\Omega$  or  $r_e^*$  (equivalently  $R$ ) is increased the wall effectively becomes more compliant. Initially a small departure from the rigid boundary is assumed by using a relatively small value for  $\Omega$  in order to assess the influence of wall compliance on the two solution branches.

Figure 4 shows the effect of this level of wall compliance at  $R = 530$  when  $\omega_i = 0.000289$ . It is shown that the branch-1 mode is stabilized, as expected from previous investigations, but particularly in the vicinity of the pinch point. The branch-3 mode, however, is moved to more negative values of  $\alpha_i$  so that the two branches diverge in comparison to the rigid-wall state. Thus the pinching process no longer occurs indicating that the compliant boundary has prevented the appearance of absolute instability at these values of  $R$  and  $\omega_i$ .

In order to assess the full effect of the compliant boundary on the absolute instability  $\omega_i$  is fixed at zero and parameters varied until a pinch point is found to occur. These parameter values then define, for the compliant boundary, the beginning of the region of absolute instability. The Reynolds number was increased, with  $\omega_i = 0$ , until a change in the character of the solution branches became evident and coalescence had occurred. From figure 5(a) it can be seen that coalescence of the two modes is delayed

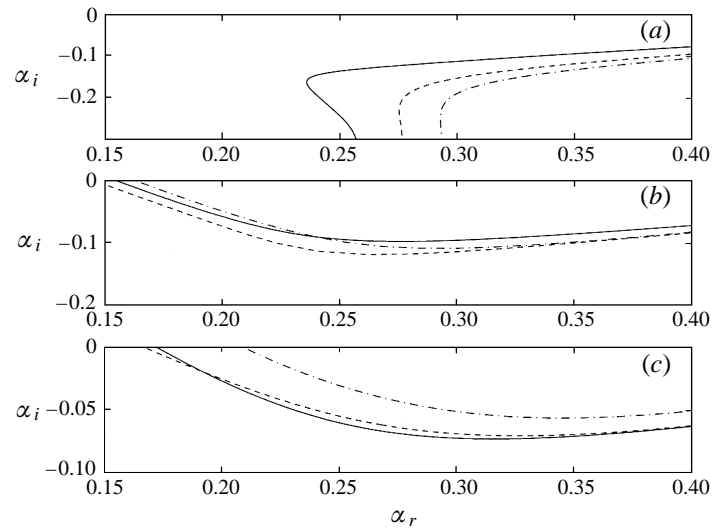


FIGURE 6. Effect of rotation rate on branch-1 mode. (a)  $\Omega = 2.5 \text{ rad s}^{-1}$ , (b)  $\Omega = 5 \text{ rad s}^{-1}$ , (c)  $\Omega = 10 \text{ rad s}^{-1}$ . —,  $R = 625$ ; - -,  $R = 850$ ; - · -,  $R = 1150$ .

until  $R \approx 607.8$ , when  $\beta = 0.126$ , so that only a small degree of wall compliance is enough to alter the delicate balance between the two solution branches and delay the onset of absolute instability. Pinching is then expected to occur at  $\omega_i > 0$ , indicating temporal growth, for  $R > 607.8$  when  $\Omega = 2.5 \text{ rad s}^{-1}$ . The onset of the absolute instability can also be seen by following the group velocity of the branch-1 mode as  $R$  is increased. Figure 5(b) shows how the group velocity falls as  $R$  becomes larger and becomes zero at  $R \approx 607.8$ . The group velocity loops below zero at higher Reynolds numbers indicating the establishment of absolute instability.

The effect of a greater degree of wall compliance on the instability characteristics was analysed by considering higher rotation rates. The effect of  $\Omega = 5$  and  $10 \text{ rad s}^{-1}$  on the solution branches at  $R = 625, 850$  and  $1150$  has been calculated. Lingwood (1995) stated that pinching occurs at larger values of  $\omega_i$  as  $R$  is increased. Evidence for this can be seen in figure 6(a), where for  $\Omega = 2.5 \text{ rad s}^{-1}$  absolute instability has already set in at these Reynolds numbers. The cusp point in the solution curve, resulting from the pinching of the two branches, disappears as  $R$  becomes larger and the curves become increasingly shallow. However, raising the level of wall compliance by raising  $\Omega$  to  $5$  and  $10 \text{ rad s}^{-1}$  produces a change in the behaviour of the solution branches. Evidence of pinching is no longer present and, significantly, branch-1 solution curves begin to move upwards in the  $\alpha$ -plane as  $R$  is increased, contrary to the pattern observed in figure 5. The group velocities associated with these results remain well above zero for all the cases examined at  $\Omega = 5$  and  $10 \text{ rad s}^{-1}$ . On the basis of these results this suggests that as  $\Omega$  is increased further coalescence of the branch-1 and -3 modes is unlikely to occur. The reason for this would appear to lie in the fact that as  $R$  and  $\Omega$  are increased the effective wall compliance is raised and the stabilizing influence on the branch-1 mode becomes proportionately greater.

Absolute instability occurs across a finite range of  $\beta$  values for the rigid wall and in order to show that the effect of wall compliance discussed above is consistent across the whole  $\beta$ -range calculations have been carried out at  $R = 850$  for two levels of wall compliance over a wide range of  $\beta$  values. Figure 7(a) shows that

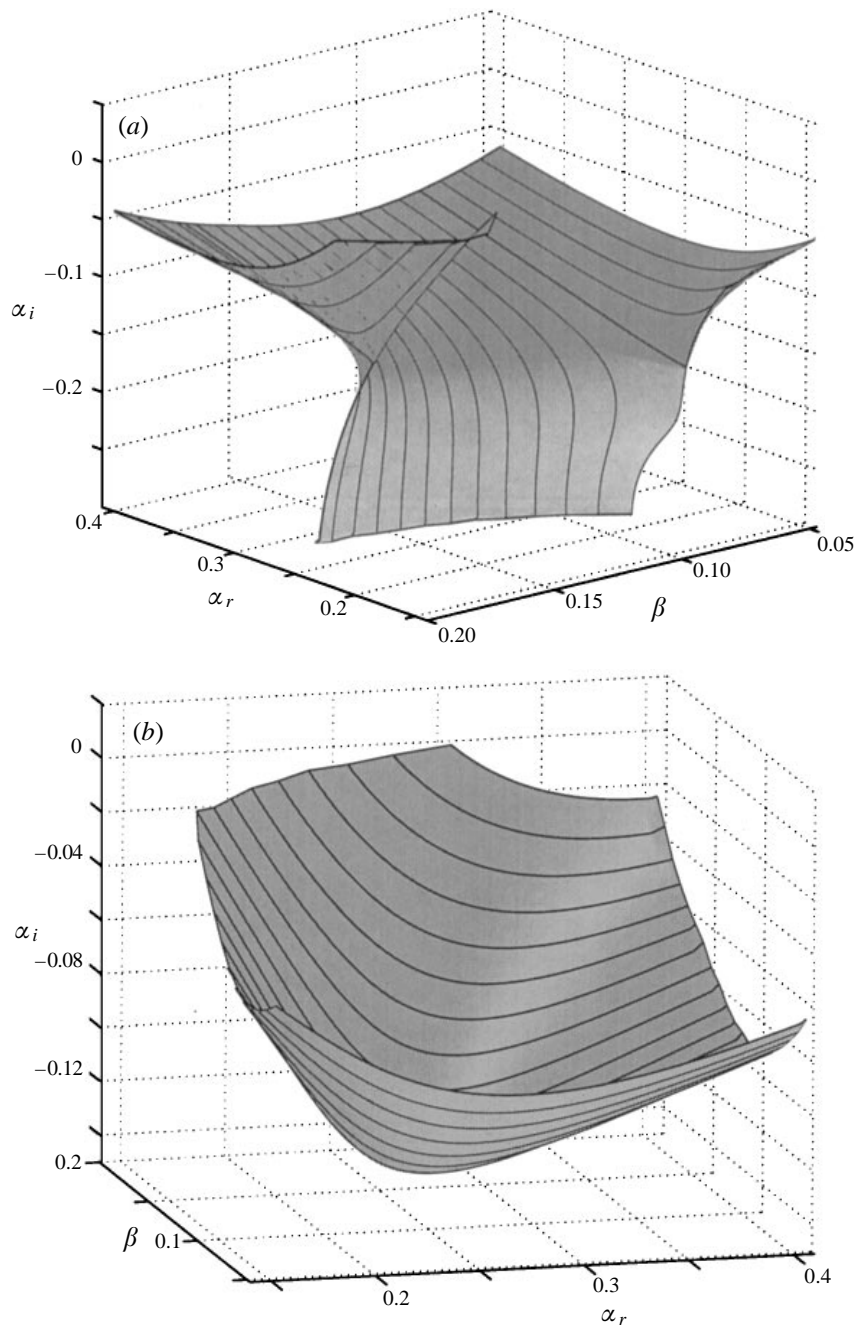


FIGURE 7. Branch-1 solutions at  $R = 850$  across the  $\beta$ -range for compliant wall. (a)  $\Omega = 2.5 \text{ rad s}^{-1}$ ; (b)  $\Omega = 5 \text{ rad s}^{-1}$ .

at  $\Omega = 2.5 \text{ rad s}^{-1}$ , absolute instability still occurs across a range of  $\beta$  values ( $0.078 < \beta < 0.171$ ). However, when  $\Omega = 5 \text{ rad s}^{-1}$ , figure 7(b) shows clearly that the branch-1 solutions retain their shape prior to coalescence which indicates the absence of absolute instability across the whole  $\beta$ -range. A critical level of wall compliance



for the azimuthal mode  $\beta = 0.126$  has been determined and it is found that  $\Omega > 4.236 \text{ rad s}^{-1}$  is sufficient to suppress the onset of absolute instability.

All the above calculations have assumed that there is no damping in the wall, so that the compliant material is purely elastic. The inclusion of wall damping, however, was found to produce no significant changes to the results presented.

#### 4. Conclusions

This study centred on the possibility of using wall compliance as a means of preventing absolute instability in the boundary layer on a rotating disc. Compliant boundaries have been used in numerous studies to reduce growth rates of convective instabilities, such as the Tollmien-Schlichting instability in the flat-plate boundary layer, with great success. In these cases wall compliance can bring about a delay in the transition process by reducing the amplification of disturbances as they propagate downstream. Absolute instability arises in the rotating-disc boundary layer as a result of the coalescence of two solutions branches of the dispersion relation. Simply reducing the growth rate of an absolute instability produces no gain in delaying transition because the breakdown process is rapid from the onset of the instability.

The full sixth-order system of governing stability equations, which include Coriolis and streamline curvature effects as well as viscous terms, was used to describe the linear stability of the fluid. This set of equations was coupled to those describing the dynamics of a single viscoelastic material layer. The results of the investigation have shown that only a low level of wall compliance suffices, theoretically, to delay the appearance of the absolute instability to higher Reynolds numbers. The process of coalescence can be suppressed leaving the flow convectively unstable. For the relatively low rotation rate of  $\Omega = 2.5 \text{ rad s}^{-1}$  (small degree of wall compliance) the Reynolds number at which absolute instability first occurs is found to rise to  $R > 607.8$  when  $\beta = 0.126$ . There is likely to be some  $\beta$  dependence but this compares to the critical value for the rigid wall of  $R > 507.3$  (Lingwood 1997*b*). A significant factor in this process is the stabilizing influence that wall compliance exerts on the branch-1 mode and the opposing effect it appears to have on the branch-3 solution. This causes the two solution curves to diverge in the  $\alpha$ -plane and delays the intersection of the two branches.

As the level of wall compliance rises the results suggest that the occurrence of absolute instability could be eliminated completely. In order to suppress the onset of absolute instability across the entire  $\beta$  range at  $R = 850$ , for example, a rotation rate of only  $5 \text{ rad s}^{-1}$  is required, which still represents a modest level of wall compliance. As  $\Omega$  is increased further the stabilizing influence of wall compliance on the branch-1 mode becomes more pronounced and the likelihood of coalescence or pinching would appear to be eradicated.

From a practical view point it is important to be aware that another type of instability can occur for flows over compliant walls. This was first analysed by Brazier-Smith & Scott (1984) for the special case of the unsupported flexible plate. Subsequently Carpenter & Garrad (1986), Lucey & Carpenter (1992) and Yeo, Khoo & Zhao (1996) have investigated absolute instability in two-dimensional flows over compliant walls. This type of instability is usually termed *divergence* and occurs when the wall becomes sufficiently compliant. It has been observed in experiments on rotating compliant discs by Hansen & Hunston (1974, 1976, 1983) and Hansen *et al.* (1980).

In conclusion, it is suggested that there exists an optimum level of wall compliance

which is sufficiently high to suppress the absolute instability formed by the coalescence of Type I and III eigenmodes, but sufficiently low to avoid the occurrence of divergence. The route to transition through absolute instability could therefore be removed with the use of a compliant boundary. Our work also suggests that an experimental study of the effects of wall compliance on the boundary-layer instabilities over a rotating disc could provide further corroboration of Lingwood's theory.

This work was supported by the EPSRC and MTD Ltd. through the award of research grants.

## REFERENCES

- BERS, A. 1975 Linear waves and instabilities. In *Physique des Plasmas* (ed. C. DeWitt & J. Peyraud), pp. 117–215. Gordon & Breach.
- BRAZIER-SMITH, P. R. & SCOTT, J. F. 1984 Stability of fluid flow in the presence of a compliant surface. *Wave Motion* **6**, 547–560.
- BRIGGS, R. J. 1964 *Electron-Stream Interaction with Plasmas*. MIT Press.
- CARPENTER, P. W. & GARRAD, A. D. 1986 The hydrodynamic stability of flow over Kramer-type compliant surfaces. Part 2. Flow-induced surface instabilities. *J. Fluid Mech.* **170**, 199–232.
- COOPER, A. J. & CARPENTER, P. W. 1997 The stability of rotating-disc boundary-layer flow over a compliant wall. Part 1. Type I and II instabilities. *J. Fluid Mech.* **350**, 231–259.
- HANSEN, R. J. & HUNSTON, D. L. 1974 An experimental study of turbulent flows over compliant surfaces. *J. Sound Vib.* **34**, 297–308.
- HANSEN, R. J. & HUNSTON, D. L. 1976 Further observations on flow-generated surface waves in compliant surfaces. *J. Sound Vib.* **46**, 593–595.
- HANSEN, R. J. & HUNSTON, D. L. 1983 Fluid-property effects on flow-generated waves on a compliant surface. *J. Fluid Mech.* **133**, 161–177.
- HANSEN, R. J., HUNSTON, D. L., NI, C. C. & REICHMANN, M. M. 1980 An experimental study of flow-generated waves on a flexible surface. *J. Sound Vib.* **68**, 317–334.
- HUERRE, P. & MONKEWITZ, P. A. 1990 Local and global instabilities in spatially developing flows. *Ann. Rev. Fluid Mech.* **22**, 473–537.
- KÁRMÁN, TH. VON 1921 Über laminare und turbulente Reibung. *Z. Angew. Math. Mech.* **1**, 233–252.
- LINGWOOD, R. J. 1995 Absolute instability of the boundary layer on a rotating disk. *J. Fluid Mech.* **299**, 17–33.
- LINGWOOD, R. J. 1996 An experimental study of absolute instability of the rotating-disk boundary-layer flow. *J. Fluid Mech.* **314**, 373–405.
- LINGWOOD, R. J. 1997a On the difficulties associated with the steepest-descent method of evaluating wave packets in unstable flows. *Stud. Appl. Maths* **98**, 213–254.
- LINGWOOD, R. J. 1997b Absolute instability of the Ekman layer and related rotating flows. *J. Fluid Mech.* **331**, 405–428.
- LUCEY, A. D. & CARPENTER, P. W. 1992 A numerical simulation of the interaction of a compliant wall and inviscid flow. *J. Fluid Mech.* **234**, 121–146.
- MACK, L. M. 1985 The wave pattern produced by point source on a rotating disk. *AIAA Paper* 85-0490.
- MALIK, M. R., WILKINSON, S. P. & ORSZAG, S. A. 1981 Instability and transition in rotating disk flow. *AIAA J.* **19**, 1131–1138.
- YEO, K. S., KHOO, B. C. & ZHAO, H. Z. 1996 The absolute instability of boundary-layer flow over viscoelastic walls. *Theor. Comput. Fluid Dyn.* **8**, 237–252.